Electrical Stimuli Release ATP to Increase GLUT4 Translocation and Glucose Uptake via PI3Kγ-Akt-AS160 in Skeletal Muscle Cells

Cesar Osorio-Fuentealba,[1] Ariel E. Contreras-Ferrat,[1] Francisco Altamirano,[1] Alejandra Espinosa,[1,2] Qing Li,[3,4] Wenyan Niu,[4] Sergio Lavandero,[1,5,6] Amira Klip,[3] and Enrique Jaimovich[1]

Skeletal muscle glucose uptake in response to exercise is preserved in insulin-resistant conditions, but the signals involved are debated. ATP is released from skeletal muscle by contractile activity and can autocrinely signal through purinergic receptors, and we hypothesized it may influence glucose uptake. Electrical stimulation, ATP, and insulin each increased fluorescent 2-NBD-Glucose (2-NBDG) uptake in primary myotubes, but only electrical stimulation and ATP-dependent 2-NBDG uptake were inhibited by adenosine-phosphate phosphatase and by purinergic receptor blockade (suramin). Electrical stimulation transiently elevated extracellular ATP and caused Akt phosphorylation that was additive to insulin and inhibited by suramin. Exogenous ATP transiently activated Akt and, inhibiting phosphatidylinositol 3-kinase (PI3K) or Akt as well as dominant-negative Akt mutant, reduced ATP-dependent 2-NBDG uptake and Akt phosphorylation. ATP-dependent 2-NBDG uptake was also inhibited by the G protein βγ subunit-interacting peptide βark-ct and by the phosphatidylinositol 3-kinase-γ (PI3Kγ) inhibitor AS605240. ATP caused translocation of GLUT4*myc*-eGFP to the cell surface, mechanistically mediated by increased exocytosis involving AS160/Rab8A reduced by dominant-negative Akt or PI3Kγ kinase-dead mutants, and potentiated by myristoylated PI3Kγ. ATP stimulated 2-NBDG uptake in normal and insulin-resistant adult muscle fibers, resembling the reported effect of exercise. Hence, the ATP-induced pathway may be tapped to bypass insulin resistance. ***Diabetes*** **62:1519–1526, 2013**

Regular exercise confers numerous health benefits, including reduced risk of developing type 2 diabetes (1,2) and lowering blood glucose in people with diabetes, partly due to an increase in the rate of glucose transport into the skeletal muscles and elevating insulin sensitivity in the postexercise period (3–6). Despite the clinical importance of the metabolic effects of exercise, the underlying molecular mechanisms that mediate these responses remain unclear.

From the [1]Center for Molecular Studies of the Cell, Biomedical Sciences Institute, Universidad de Chile, Santiago, Chile; the [2]School of Medical Technology, Faculty of Medicine, Universidad de Chile, Santiago, Chile; the [3]Cell Biology Program, The Hospital for Sick Children, Toronto, Ontario, Canada; the [4]Department of Immunology, Tianjin Medical University, Tianjin, China; the [5]Faculty of Pharmaceutical and Chemical Sciences, Universidad de Chile, Santiago, Chile; and the [6]Department of Internal Medicine (Cardiology), University of Texas Southwestern Medical Center, Dallas, Texas.

Corresponding author: Enrique Jaimovich, ejaimovi@med.uchile.cl.

Received 7 August 2012 and accepted 9 November 2012.

DOI: 10.2337/db12-1066

This article contains Supplementary Data online at http://diabetes.diabetesjournals.org/lookup/suppl/doi:10.2337/db12-1066/-/DC1.

C.O.-F. and A.E.C.-F. contributed equally to this work.

Exercise and insulin are the most important physiological stimuli to increase glucose transport into skeletal muscle fibers (5,7). Each stimulus results in redistribution of GLUT4 from the muscle cell interior to surface membranes, which ultimately leads to a larger glucose transport rate into the muscle cell (8–10). The proposed mechanisms through which a single bout of physical exercise increases glucose transport in skeletal muscle involve intracellular signal transduction that is distinct from that of insulin (5,11). The putative exercise-derived signals have long been elusive, but a need for intracellular Ca^{2+} below the threshold needed to evoke contraction was early recognized (12,13). AMP-activated protein kinase (AMPK) has been proposed as a mediator of insulin-independent glucose transport in skeletal muscle (14–16). Although AMPK is a master regulator of metabolic and transcriptional functions in tissues and cells throughout the body during exercise (17), its role in contraction-stimulated glucose transport has been questioned (18,19).

We previously reported that tetanic electrical stimulation of skeletal myotubes evokes a fast Ca^{2+} transient related to excitation–contraction coupling (20) and a slow Ca^{2+} transient, within seconds of stimulus initiation (21), that was not related to excitation-contraction coupling (22). The fast transient arises from Ca^{2+} release from ryanodine-sensitive stores, whereas the slow component is Ca^{2+} released through inositol-1,4,5-trisphosphate receptor (IP3R) (21,23) and depends on ATP concomitantly released from the stimulated cells (24). ATP signals in skeletal muscle through P2Y and P2× purinergic receptors (24), G-protein–coupled receptors that typically signal through the βγ subunits to activate phosphatidylinositol 3-kinase-γ (PI3Kγ) (21). We therefore hypothesized that extracellular ATP may signal through PI3Kγ and further downstream to Akt. Because Akt phosphorylation is a key regulator of GLUT4 traffic, ATP may ultimately stimulate glucose uptake through this transporter. Here we describe that in primary and L6 myotubes as well as in adult muscle fibers, electrical stimulation and ATP indeed signal through PI3Kγ downstream to Akt and its substrate AS160 and mobilize GLUT4 to the surface via Rab8-mediated exocytosis and decreased endocytosis to increase glucose uptake.

RESEARCH DESIGN AND METHODS

Reagents. ATP, ADP, UTP, and apyrase grade VII from potato, suramin, cytosine arabinoside, penicillin-streptomycin, nifedipine, and amphotericin B were obtained from Sigma-Aldrich (St. Louis, MO). Dulbecco's modified Eagle's medium-F12, bovine serum, and FBS, were from Invitrogen (Grand Island, NY). Collagenase type II and IV were from Worthington Biochemical Corp. (Lakewood, NJ). Mini protease inhibitors were from Roche Applied Science

(Manheim, Germany). Secondary horseradish peroxidase (HRP)-conjugated anti-rabbit and anti-mouse antibodies were from Pierce Biotechnology (Rockford, IL). Enhanced chemiluminescence reagents were from Amersham Biosciences (Piscataway, NJ). Polyvinylidene difluoride (PVDF) membranes were from Millipore (Bedford, MA). All other reagents were obtained from Sigma-Aldrich, Merck (Darmstadt, Germany), or Invitrogen. 2-NBD-Glucose (2-NBDG) and anti-rabbit Alexa 546 were from Molecular Probes (Eugene, OR). LY-294002, Akt inhibitor VIII, and AS605240 were from Calbiochem (La Jolla, CA). Anti-*myc* polyclonal antibody was from Sigma-Aldrich. pAkt (Thr308, Ser473), anti-IRβ (Tyr1150/1151), pAS160, and total AS160 were from Cell Signaling Technology (Danvers, MA). Ser318, Ser341, Ser570, Ser588, and Thr 751 were provided courtesy of Dr. James Hastie (Division of Signal Transduction, University of Dundee). Rab8A and Rab10 (Santa Cruz Biotechnology, Santa Cruz, CA), Actinin I (Sigma), Rab8A small interfering RNA (siRNA; Qiagen, Mississauga, Ontario, Canada) sequence: CAGCGCGAAGGCCAACATCAA; Rab10 siRNA (Qiagen) sequence: AACGATTTCACACCATCACAA; and NR 2 Sequence: AATAAGGCTATGAAGAGATAC.

Animals. Newborn rats and C57BL/6 mice were bred in the Animal Breeding Facility, Faculty of Medicine, University of Chile. Studies were approved by the Institutional Bioethical Committee, Faculty of Medicine, University of Chile, in accordance with the "Guide for the Care and Use of Laboratory Animals," National Institutes of Health (NIH).

Cell cultures. Primary cultures of skeletal muscle cells were prepared from Sprague-Dawley neonatal rats as previously reported (22), or using α-minimum essential medium containing 5.5 mmol/L glucose. Cultures used were 6 to 7 days old. L6 muscle cells stably expressing GLUT4 with a *myc* epitope in the first extracellular loop (L6-GLUT4*myc*) were cultured, as described previously (25). L6-GLUT4*myc* myoblasts stably expressing human AS160 were generated (cDNA donated by Dr. G.E. Lienhard, Dartmouth Medical School, NH). L6-GLUT4*myc* cells were transfected with siRNAs for Rab8A or Rab10 using jetPrime, Polyplus-Transfection (New York, NY), incubated for 24 h, and then cultured for 48 h. Primary fibers of flexor digitorum brevis muscle were prepared from C57BL/6 mice, as previously described (26). Male mice were fed ad libitum a standard chow diet, which provides 20% protein, 10% fat and 70% carbohydrate, or a high-fat diet D12492 (Research Diets Inc., New Brunswick, NJ) from 21 days after birth for 8 weeks.

Cellular treatments. Cells were washed with Ca^{2+} and Mg^{2+}-free PBS and maintained under resting conditions for 30 min in Krebs-Ringer phosphate-HEPES glucose buffer [in mmol/L: 20 HEPES-Tris (pH 7.4), 118 NaCl, 4.7 KCl, 3 $CaCl_2$, 1.2 $MgCl_2$, and 10 glucose]. For immunoblotting, cells were stimulated with 100 nmol/L insulin or 100 μmol/L ATP, and the medium was changed immediately after. For electrical stimulation, a single tetanus (45 Hz, 400 pulses of 1-ms duration) was applied, after which cells were lysed or studied for glucose uptake. Cells were incubated with pharmacological inhibitors for 30 min and stimulated in the presence of each inhibitor. DMSO or ethanol were kept <0.1%.

Protein immunodetection. Western blotting was performed as previously reported (27). We used anti–p-Akt (1:1,000); anti-Akt (1:1,000); anti-IRβ (Tyr1150/1151; 1:1,000); β-actin (1:3,000), AS160 total (1:1,000), pAS160 Ser341, Ser570, Ser588, and Thr 751 (1:1,000) for overnight incubations at 4°C. After secondary antibody addition, membranes were developed by enhanced chemiluminescence according to the manufacturer's instructions. For the loading control, anti-Akt or anti-β actin were used. Densitometry analysis was performed with ImageJ software (NIH, Bethesda, MD).

^{3}H-2DG uptake. Myotubes were grown and differentiated in 12-well plates (10^6 cells/well). Before the indicated experiments, cells were preincubated with suramin for 30 min at 37°C in Dulbecco's modified Eagle's medium. Insulin or ATP was added when needed for 15 min at 37°C. Myotubes were rinsed twice with HEPES-buffered saline solution [in mmol/L: NaCl 122, KCl 4.9, $MgSO_4$ 2.5, $CaCl_2$ 1, HEPES 20 (pH 7.4)], and carrier-mediated glucose uptake was measured for 10 min using 10 μmol/L ^{3}H-2-deoxyglucose in the above solution at 37°C with or without indinavir. Myotubes were rinsed three times with ice-cold HEPES-buffered saline solution containing D-glucose (30 mmol/L). Trapped radioactivity was determined by liquid scintillation counting after addition of 0.05N NaOH. Noncarrier-mediated uptake was measured in parallel incubations using cytochalasin B (5 μmol/L) in the transport solution.

Single-cell fluorescent hexose uptake assay. Myotubes were washed with Krebs-Ringer buffer and stimulated with insulin or ATP. Cells were exposure to 2-NBDG (300 μmol/L) for 15 min, rinsed with Krebs buffer, and transferred to a confocal Carl Zeiss Pascal 5 microscope and PlanApofluo (original magnification ×40; numerical aperture, 1.3). Cultures were excited at 488 nm and the fluorescence was captured at 505–550 nm band-pass filter emission. Hexose uptake was estimated by comparing intracellular fluorescence with the extracellular signal. For each condition, 100 cells were analyzed in each culture were used. Images were quantified by ImageJ software (NIH, Bethesda, MD).

Extracellular nucleotide measurement. The extracellular medium was replaced by 1.5 mL Krebs buffer 1 h before nucleotide assay. For whole-dish electrical stimulation, we built a device consisting of a row of six platinum wires 1-cm apart with alternate polarity across a circular plastic holder that fits the dish. Cells were stimulated with a tetanus protocol and extracellular aliquots were removed 0 to 30 min poststimulus. Cells from each plate were lysed, and proteins were quantified using Coomassie Plus protein assay (Pierce, Rockford, IL). Data are expressed as picomoles of extracellular nucleotide per milligram of protein.

ATP detection by luciferase assay. Fifty microliters of extracellular samples were added to 20 μL CellTiter-Glo luminescent cell viability assay (Promega, Madison, WI). After a 10-min incubation in the dark, samples were quantified in a luminometer. In parallel, a standard curve from 1 fmol to 100 pmol ATP was performed using the same kit. Linearity was observed between 100 fmol and 10 pmol.

Recombinant adenoviruses. Adenoviruses (Ad) for myristoylated Akt (AdAkt-myr), dominant-negative Akt (AdAkt-dn), and an empty construct (Ad-empty) were a gift from Dr. Joseph A Hill (University of Texas Southwestern Medical Center, Dallas, TX). Transduction efficiency was >95%, monitored with green fluorescent protein (GFP)-encoded recombinant adenovirus. Myotubes were infected with adenoviral vectors at a multiplicity of infection of 5,000 at least 48 h before experiments.

Cell-surface GLUT4*myc* quantification. This assay was previously described (25) and here termed the OPD assay (for *o*-phenylenediamine). Briefly, cells were stimulated and washed twice with ice-cold PBS, fixed with 4% (v/v) paraformaldehyde for 15 min, quenched with 100 mmol/L glycine for 10 min, and blocked with 5% (v/v) goat serum. Myotubes were incubated with polyclonal anti-*myc* antibody (1:500) for 2 h at 4°C, then washed with PBS and incubated with HRP-bound goat anti-rabbit secondary antibody (1:1,000) for 1 h at 4°C. OPD reaction was carried out at room temperature.

GLUT4*myc* endocytosis and re-exocytosis. GLUT4*myc* internalization and re-exocytosis were measured as previously described (28). Treatments with insulin and ATP were applied to cells before and after antibody labeling.

Plasmids transfections and immunofluorescence microscopy. Myotubes were transfected with 3 μg GLUT4*myc*-eGFP (29) PI3Kγ-wild-type, PI3Kγ-kinase dead, PI3Kγ-myr (donated by Dr. T.R. Jackson, University of Newcastle, U.K.) using 6 μL/mL Lipofectamine 2000 (Invitrogen). Transfection efficiency was ~15%. Myotubes were incubated with transfection mixture for 4 h in OPTI-MEM (Invitrogen) media, incubated in F12- Dulbecco's modified Eagle's medium (1:1) for 36 h, and stimulated and processed. Cell surface GLUT4*myc*-eGFP was determined as described (29).

Statistical analysis. Data were expressed as mean ± SD. Statistical differences between two groups of data were analyzed by Student *t* test. For multiple comparisons, one-way ANOVA was used, followed by Bonferroni post-test analysis, as appropriate. $P < 0.05$ was considered statistically significant.

RESULTS

Electrical stimulation-dependent 2-NBDG uptake requires purinergic receptors and extracellular nucleoside phosphate. Single myotubes analysis was performed to study the effects of electrical stimuli, ATP, and insulin on the uptake of the nonmetabolizable fluorescent glucose analog 2-NBDG (Fig. 1*A*). Moderate tetanic stimulation (45Hz, 400 1-ms pulses lasting 9 s) induced an increase in 2-NBDG uptake (2.50 ± 0.55-fold), as did 100 μmol/L ATP (2.73 ± 0.52-fold) or 100 nmol/L insulin (2.87 ± 0.41; Fig. 1*A* and *B*). A significant increase was observed with 50 μmol/L external ATP (Supplementary Fig. 1*A*), and it peaked with 100 μmol/L. While primary myotubes were regularly grown in medium containing 25 mmol/L glucose, insulin, and ATP, similarly stimulated myotubes were cultured in 5.5 mmol/L (Supplementary Fig.1*B*). Exogenously added ADP or UTP also elevated 2-NBDG uptake (Supplementary Fig. 1*C*). Preincubation with 2 units/mL apyrase, which catalyzes the hydrolysis of both ATP and ADP, did not affect basal 2-NBDG uptake but eliminated the increase evoked by electrical stimulus (Fig. 1*C*). In addition, pretreatment with the purinergic receptor inhibitor suramin (100 μmol/L) inhibited electrical stimulus-dependent 2-NBDG uptake, without affecting basal uptake (Fig. 1*D*). Furthermore, apyrase (Fig. 1*E*) and suramin (Fig. 1*F*) both blocked ATP-dependent 2-NBDG uptake,

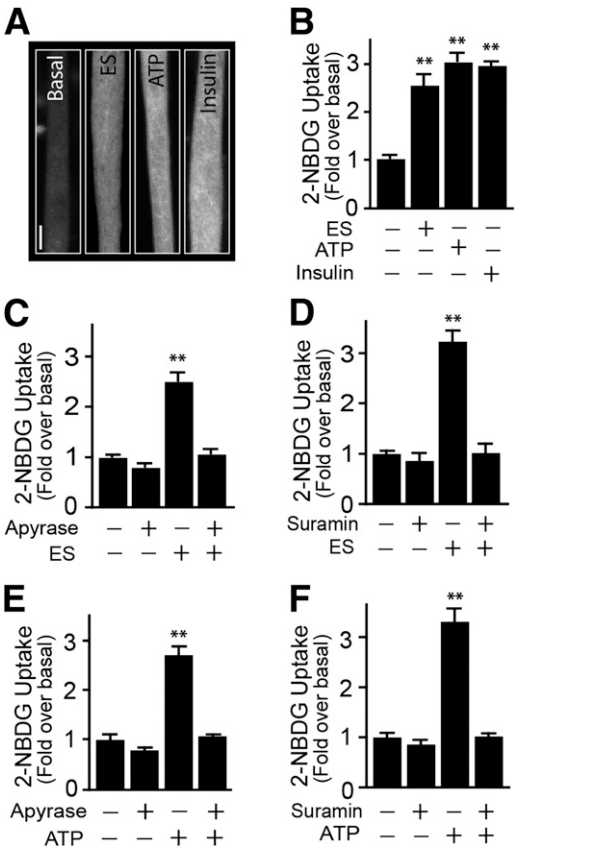

FIG. 1. Electrical stimulation (ES) induces ATP-dependent glucose uptake in myotubes. Primary myotubes were exposed to tetanic stimulation (400 pulses, 1-ms each at 45 Hz), insulin (100 nmol/L), or exogenous ATP (100 μmol/L). 2-NBDG uptake was assayed as indicated in RESEARCH DESIGN AND METHODS. *A*: Representative image of 2-NBDG uptake induced by ES, ATP, or insulin, measured 15 min after stimulation. *B*: 2-NBDG uptake quantification. Myotubes were preincubated for 30 min with or without apyrase (2 units/mL) (*C*) or suramin (100 μmol/L) (*D*), and electrically stimulated. Myotubes were preincubated for 30 min with or without apyrase (2 units/mL) (*E*) or suramin (100 μmol/L) (*F*) and then treated with exogenous ATP. Values represent the mean ± SD. ***P* < 0.001 vs. basal group. Data are from at least five independent experiments corresponding to 90 cells analyzed per condition. Scale bar: 10 μm.

without affecting insulin-dependent uptake (Supplementary Fig. 2*E*).

The stimulation of 2-NBDG uptake was corroborated in monolayers of myotubes using the conventional ^{3}H-2DG uptake. Insulin or ATP each caused an increase in glucose uptake, measured after 20 min. Suramin strongly reduced ATP-dependent glucose uptake without affecting basal uptake (Supplementary Fig. 1*D*). Cytochalasin B, an inhibitor of class I GLUT activity (primarily GLUT1, 3, 4), completely abolished basal and insulin-dependent glucose uptake (Supplementary Fig. 1*E*), whereas Indinavir, an effective GLUT4 inhibitor (30) also significantly decreased ATP-dependent glucose uptake, without affecting basal glucose uptake (Supplementary Figs. 1*D* and 2*C*). Of note, neither insulin nor ATP stimulated glucose uptake in muscle-derived primary cultures of fibroblasts (data not shown).

Electrical stimulus increases extracellular ATP, activating Akt and the GAP-Rab AS160. We measured ATP in the medium after tetanic stimulation. A transient ATP increase was significant by 30 s and reached maximal levels by 1 min (Fig. 2*A*). Unlike insulin, exogenously added ATP did not affect insulin receptor phosphorylation (Supplementary Fig. 2*A*), indicating that ATP-induced glucose uptake occurs via an insulin receptor-independent pathway. However, downstream signals may be common to both insulin and ATP. Interestingly, tetanic stimulation of myotubes provoked an increase in Akt phosphorylation, and this response was abrogated by inclusion of suramin in the medium before and during stimulation (Fig. 2*B*). This finding suggests that purinergic receptors may be activated by electrical stimulation and lead to Akt activation. Maximal stimulation of Akt phosphorylation occurred 30 min after the electrical stimulation and decreased by 60 min (Supplementary Fig. 2*B*).

Exogenously added ATP also stimulated Akt phosphorylation at Thr308 and Ser473 to levels comparable to those induced by insulin (Fig. 2*C*). Insulin-activated Akt leads to phosphorylation of the GAP-Rab AS160, an event required for GLUT4 translocation. Like insulin, ATP strongly induced phosphorylation of AS160 at Thr751, Thr642, Ser588, Ser570, Ser341, and Ser318 (Fig. 2*D*). Moreover, exposing myotubes to electrical stimulation followed by insulin, produced an additive effect on Akt activation but not when the order was reversed (Fig. 2*E*). It is possible that the effect of a high dose of insulin may saturate the

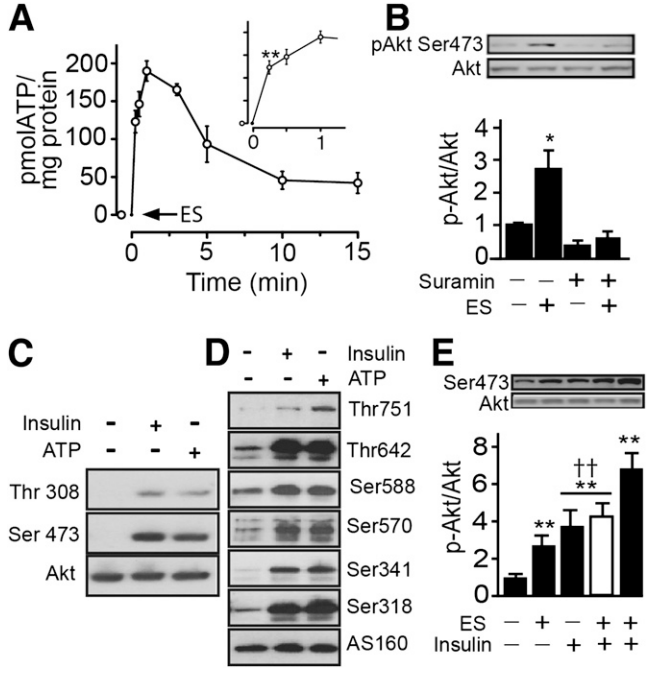

FIG. 2. Electrical stimulation (ES) induces ATP-dependent Akt-AS160 phosphorylation in skeletal muscle cells. *A*: Primary myotubes were electrically stimulated, then aliquots of the extracellular medium were removed at the indicated times. ATP was measured by the luciferin/luciferase assay and quantified against a standard curve, as indicated in RESEARCH DESIGN AND METHODS. Cell lysates were analyzed for pAkt, total Akt, pAS160, and total AS160. *B*: Primary myotubes were preincubated for 30 min, with or without suramin (100 μmol/L), followed by assay of Akt phosphorylation at Ser473. *C*: L6-GLUT4*myc*-AS160 muscle cells were stimulated with exogenous ATP (100 μmol/L) or insulin (100 nmol/L) for 5 min, and then Akt phosphorylation at Thr308 and Ser473 was measured. *D*: L6-GLUT4*myc*-AS160 myoblasts were stimulated with exogenous ATP (100 μmol/L) or insulin (100 nmol/L) for 5 min, and then AS160 phosphorylation at Thr751, Thr642, Ser588, Ser570, Ser341, Ser318, and total AS160 was measured. *E*: Primary myotubes were electrically stimulated or treated with insulin (100 nmol/L), or both, for 5 min. The white bar shows insulin stimulation for 5 min and then electrical stimulation, and the black bar shows electrical stimulation first and then insulin stimulation for 5 min. Values represent the mean ± SD. ***P* < 0.001, **P* < 0.01 vs. basal group. ††*P* < 0.001. Data are from at least three independent experiments.

same Akt pool that is targeted by electrical stimulation, whereas tetanic stimulation does not. Further experiments are needed to ascertain whether a fast turnover rate of phospho-Akt after electrical stimuli or recruitment of an additional pool could explain the additive effect of insulin in these conditions.

ATP-dependent glucose uptake involves the PI3K-Akt axis. The general PI3K inhibitor, LY-294002 (50 μmol/L) abrogated the effect of insulin but only partly reduced ATP-induced Akt phosphorylation (Supplementary Fig. 2*D*). Similarly, LY-294002 eliminated the stimulation by insulin of 2-NBDG uptake but incompletely reduced ATP-dependent stimulation by 70% (Fig. 3*A*). Unlike a more complete inhibition of insulin action, the specific Akt inhibitor $Akt_i1/2$ (10 μmol/L) only partially inhibited ATP-dependent 2-NBDG uptake (Fig. 3*B*). These results suggest that ATP and insulin do not trigger identical signaling mechanisms.

The participation of Akt was further investigated by transducing primary myotubes with adenovirus encoding AdAkt-dn [multiplicity of infection (MOI) 5,000] or, as positive control, constitutively active AdAkt-myr (MOI 5,000). Empty vector was used as transduction control (Ad-empty, MOI 5,000). The ATP-dependent 2-NBDG uptake recorded in myotubes transduced with Ad-empty was similar to that in nontransduced cells. In contrast, myotubes infected with AdAkt-dn exhibited a decrease in the ATP response. Overexpression of Akt-myr elevated basal 2-NBDG uptake sevenfold over the nontransfected control, and ATP did not have a further stimulatory effect (Fig. 3*C*).

ATP promotes GLUT4 translocation to the cell surface. To visualize GLUT4 exposure at the plasma membrane, we transiently transfected cDNA encoding a GLUT4*myc*-eGFP chimera. Confocal slices (0.7 μm) and whole cell z stacks were imaged. In the basal state, myotubes showed GLUT4*myc* vesicles in the cytoplasm and perinuclear regions with a low surface *myc* epitope signal (Fig. 4*A*). By comparison, ATP-stimulated myotubes showed an increase in exofacially exposed *myc* epitope (Fig. 4*A*), akin to that evoked by insulin (data not shown). Cotransfection with Akt-dn plasmid lowered this gain without affecting the basal levels of surface GLUT4*myc*-eGFP (Fig. 4*A*). ATP increased the *myc*:eGFP ratio by 2.50 ± 0.3 relative to nonstimulated cells, whereas the basal *myc*:eGFP ratio was 0.82 ± 0.06 in Akt-dn cotransfected myotubes, and ATP raised this value to only 1.48 ± 0.15-fold above the basal control (Fig. 4*B*). However, cotransfection of Akt-myr plasmid evoked a maximal GLUT4*myc* surface exposure in nonstimulated myotubes. ATP-stimulated myotubes did not show any additional increase of surface *myc* epitope, indicating that the response had peaked (data not shown). These results suggest that ATP causes GLUT4*myc* translocation to cell surface by a mechanism that involves Akt activation.

ATP-dependent glucose uptake and GLUT4 translocation in myotubes require PI3Kγ activation. Overexpression of βark-ct (inhibitor of βγ subunits) partially abolished ATP-dependent 2-NBDG uptake (Fig. 5*A*), and AS 605240, a specific inhibitor of PI3Kγ, efficiently inhibited the ATP effect (Fig. 5*A*). We cotransfected GLUT4*myc*-eGFP along with different PI3Kγ mutants to evaluate the participation of PI3Kγ in GLUT4 translocation to the cell surface. Myotubes cotransfected with wild-type PI3Kγ and stimulated with ATP show a significant increase in surface GLUT4*myc* compared with control, ATP-stimulated cells (Fig. 5*B*). Conversely, cotransfection of GLUT4*myc* with

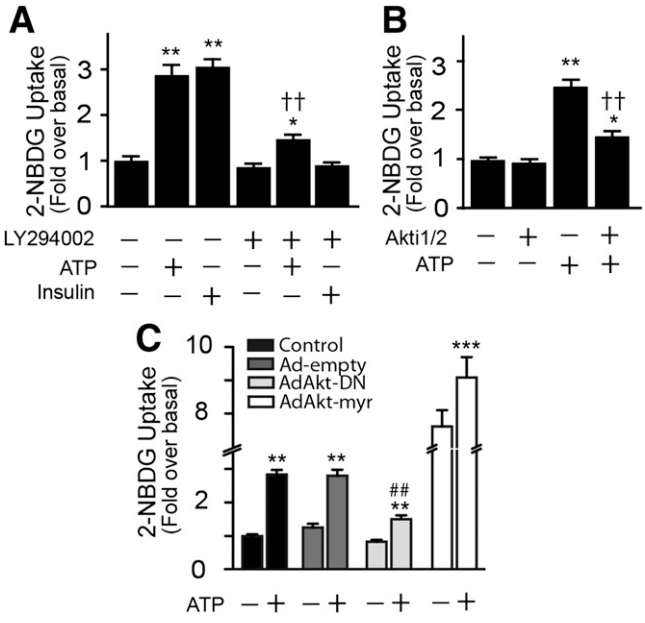

FIG. 3. ATP-dependent glucose uptake requires the PI3K-Akt axis. *A* and *B*: 2-NBDG uptake was measured in primary myotubes preincubated for 30 min with or without LY294002 (40 μmol/L) or Akt 1/2 inhibitor (10 μmol/L). *C*: Myotubes were transiently transduced with AdAkt-dn, AdAkt-myr, or Ad-empty, and 2-NBDG uptake was assayed. Values represent the mean ± SD. **$P < 0.001$, *$P < 0.01$ vs. basal group; ††$P < 0.001$ relative to ATP-treated cells; ##$P < 0.001$ relative to the control group; and ***$P < 0.05$ relative to nonstimulated. Data are from at least four independent experiments.

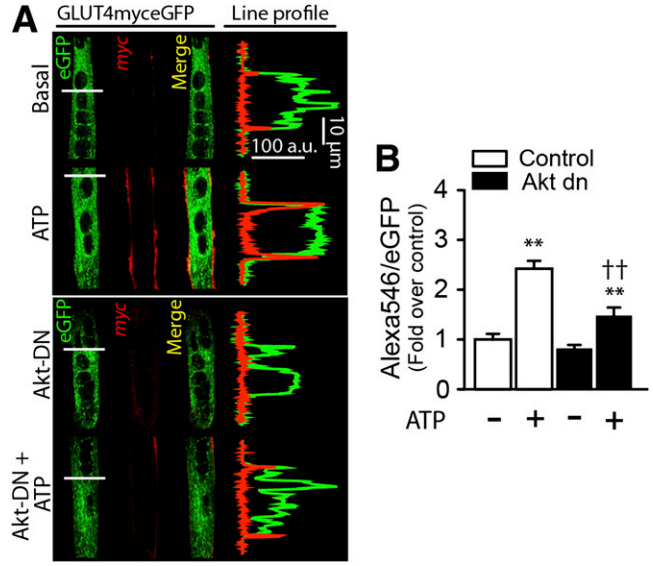

FIG. 4. ATP-promoted GLUT4*myc* translocation to the cell surface requires Akt. Primary myotubes were transiently cotransfected with GLUT4*myc*-eGFP and Akt-dn cDNA for 24 h and then stimulated with 100 μmol/L ATP for 10 min. Extracellular exposure of the *myc* epitope was detected by immunofluorescence in nonpermeabilized cells as described in RESEARCH DESIGN AND METHODS. Z stack images were collapsed in a single slice (z projection) and results expressed as the ratio of the fluorescence of surface-labeled GLUT4*myc* (red, Alexa 546) to the fluorescence of total GLUT4 expressed (green GFP). *A*: Exogenous ATP induced an increase in the Alexa 546-to-eGFP ratio. This ratio was reduced significantly in myotubes cotransfected with GLUT4*myc*-eGFP and Akt-dn. *B*: Quantification of panel A. Values are the mean ± SD. **$P < 0.001$ vs. basal group. ††$P < 0.01$ relative to ATP stimulation in the control condition. Data are from at least four independent experiments.

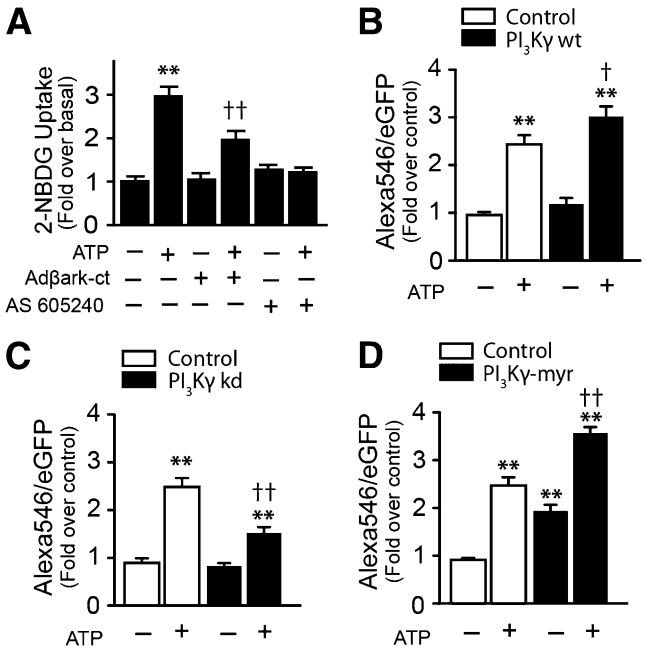

FIG. 5. ATP-dependent glucose uptake and GLUT4*myc* translocation require PI3Kγ and Gβγ activation. Skeletal myotubes were pre-incubated with PI3Kγ inhibitor AS6052540 (30 nmol/L) for 30 min or transduced with Adβark-ct (MOI 5000) for 48 h and then stimulated with ATP, as indicated. *A*: 2-NBDG uptake. *B*, *C*, and *D*, GLUT4*myc* translocation in myotubes overexpressing wild type (wt), kinase dead (kd), or PI3Kγ-myr. Values represent the mean ± SD. ***P* < 0.001 vs. basal group, †*P* < 0.01, and ††*P* < 0.001 relative to the ATP-stimulated control condition. Data are from at least four independent experiments.

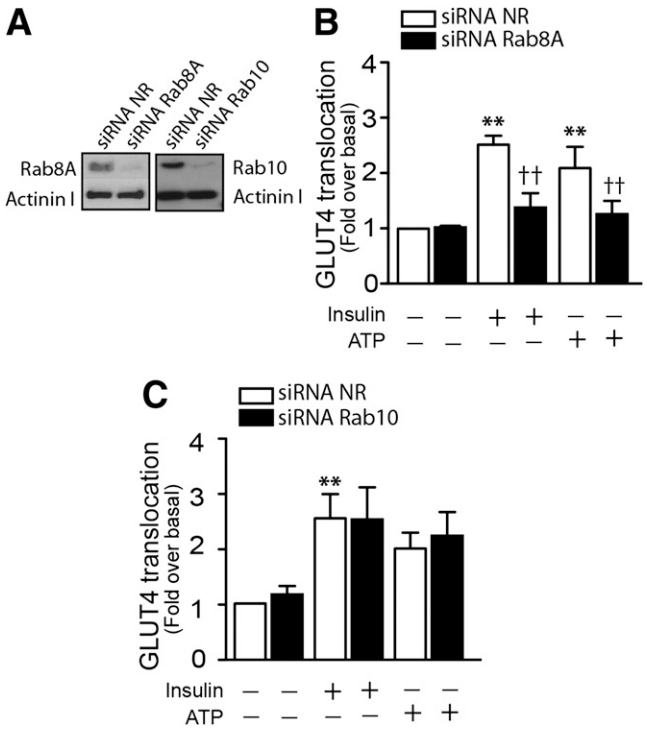

FIG. 6. ATP signaling toward AS160 and Rab8A in L6-GLUT4*myc* cells. L6 cells that stably expressed GLUT4*myc* were transiently transfected with siRNAs, as indicated in RESEARCH DESIGN AND METHODS. *A*: Rab8A and Rab10 knockdown. L6-GLUT4*myc* myoblasts were transfected with siRNA to Rab8A, to Rab10, or with nonrelated (NR) siRNA. Extracellular exposure of the *myc* epitope was detected in nonpermeabilized cells as described in RESEARCH DESIGN AND METHODS. *B* and *C*: Quantification of the effect of Rab8A or Rab10 knockdown on ATP-induced GLUT4*myc* translocation. Values are the mean ± SD. ***P* < 0.001 vs. basal group, ††*P* < 0.001 relative to the corresponding siRNA NR condition. Data are representative of at least three independent experiments.

the kinase dead form of PI3Kγ strongly decreased the effect of ATP on surface GLUT*myc* (Fig. 5*C*). Finally, in myotubes cotransfected with PI3K-myr, a myristoylated (constitutively active) form of PI3Kγ, the surface GLUT4-*myc* signal was increased in basal relative to the control condition, and as in Fig. 5*B*, the stimulating effect of ATP is still seen, possibly indicating that a larger PI3K pool is present in these conditions (Fig. 5*D*).

ATP signaling downstream of Akt toward AS160 and Rab8A. In response to insulin, Akt-AS160 phosphorylation allows manifestation of the activity of its target Rab guanosine triphosphatases leading to GLUT4 translocation to the membrane. The pertinent Rabs in L6 muscle cells are Rab8A and Rab13 (31), and Rab10 prevails in 3T3-L1 adipocytes (32,33). Because AS160 is phosphorylated in response to ATP in muscle cells, we examined the possible participation of its target Rabs in ATP-mediated glucose uptake. In L6 muscle cells stably expressing GLUT4*myc* (L6-GLUT4*myc*), ATP again caused an increase in the exofacial exposure of the *myc* epitope that was significant by 2 min and achieved a comparable level to that evoked by insulin (Supplementary Fig. 3). Knockdown of Rab8A by 80% caused significant inhibition of insulin- or ATP-dependent GLUT4*myc* translocation to cell surface (Fig. 6*A* and *B*). In contrast, similar knockdown of Rab10 did not affect the insulin- or ATP-dependent GLUT4*myc* translocation (Fig. 6*C*). Together, these data suggest participation of the Akt-AS160-Rab8A axis in ATP-dependent GLUT4 translocation and glucose uptake.

ATP-dependent GLUT4 translocation to cell surface involves a rise in GLUT4 exocytosis and a drop in GLUT4 endocytosis. To ascertain if the increase in surface GLUT4*myc* arises from exocytic vesicles similar to those promoted by insulin, primary myotubes were transiently cotransfected with GLUT4*myc*-eGFP and tetanus toxin light chain (TeTx). This toxin proteolytically cleaves vesicle-associated membrane protein 2 (VAMP2), a key v-SNARE mediating docking and fusion of insulin-sensitive GLUT4-storage vesicles (GSV) with the plasma membrane (25,34). Under basal conditions (absence of ATP), surface GLUT4*myc* was practically undetectable (Fig. 7*A*). The whole-cell quantification of GLUT4*myc* is shown for each condition (Fig. 7*B*). ATP caused a clear increase in surface *myc* epitope signal, and this response diminished in myotubes expressing TeTx (Fig. 7*A*).

The rates of exocytosis and endocytosis of GLUT4*myc* were investigated in L6-GLUT4*myc* muscle cells, a system amenable to these determinations because they require large numbers of homogeneously labeled cells (25). ATP reduced GLUT4*myc* endocytosis compared with insulin-stimulated or untreated cells (Fig. 7*C*). The rate of exocytosis was then determined after allowing surface GLUT4*myc* loaded with anti-*myc* antibody to internalize and equilibrate with intracellular GLUT4 pools before insulin stimulation. ATP caused a significant increase in GLUT4*myc* externalization, noticeable by 2 min, resembling the effect of insulin (Fig. 7*D*). Exocytosis likely involves GSV that rely on VAMP2 for fusion, as is the case of insulin-regulated GSV.

Exogenous ATP increase 2-NBDG uptake in adult muscle fibers from normal and insulin-resistant mice. ATP (100 μmol/L) induced a significant increase in 2-NDBG uptake in adult fibers isolated from flexor digitorum

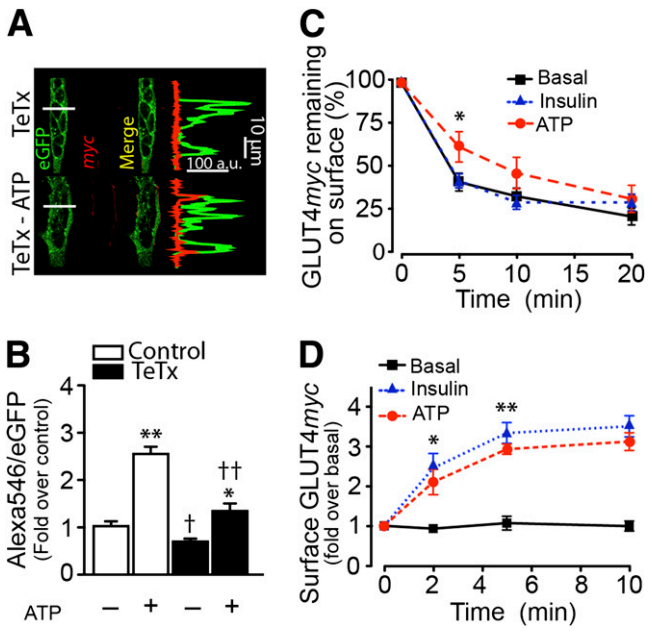

FIG. 7. ATP-dependent GLUT4*myc* translocation requires VAMP2 and reduces GLUT4*myc* endocytosis. *A* and *B*: Primary myotubes were transiently cotransfected with GLUT4*myc*-eGFP and TeTx cDNA for 24 h and then stimulated with 100 μmol/L ATP for 10 min. *C*: GLUT4*myc* endocytosis in L6-GLUT4*myc* cells. Surface GLUT4*myc* was labeled with anti-*myc* antibody, followed by extensive washing with PBS. The surface-labeled GLUT4*myc* was then allowed to internalize by rewarming for different times in presence or absence of the respective stimulus. At the indicated times, the amount of GLUT4*myc* remaining at the cell surface was determined and expressed as a percentage of the cell surface level at 0 min of endocytosis. *D*: GLUT4*myc* re-exocytosis in L6-GLUT4*myc* cells. Cells were first stimulated with 100 nmol/L insulin for 10 min to induce GLUT4*myc* translocation. Surface GLUT4*myc* was labeled with anti-*myc* antibody, followed by extensive washing with PBS, and then warmed to 37°C for 2 h to induce endocytosis in α-minimum essential medium. L6-GLUT4*myc* cells were then stimulated with exogenous ATP or insulin for 10 min. Subsequently, cells were again cooled to 4°C, and antibody-laden GLUT4*myc* was determined at the cell surface. Values are the mean ± SD. ***P* < 0.001, **P* < 0.01 vs. basal group. †*P* < 0.01 with respect to unstimulated control. ††*P* < 0.001 with respect to ATP-stimulated cells. Data are from at least four independent experiments.

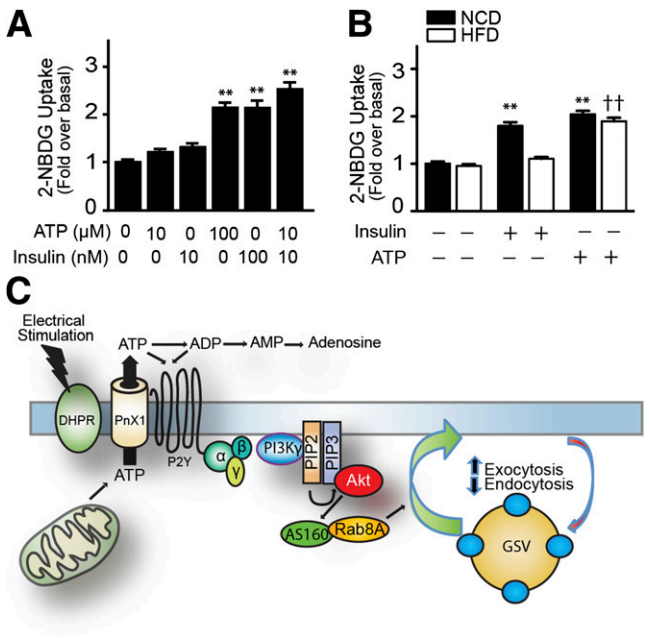

FIG. 8. Exogenous ATP increased glucose uptake in adult muscle fibers derived from control mice fed a normal-chow diet (NCD) and mice fed a high-fat diet (HFD). Proposed model for ATP-mediated glucose uptake. *A*: Fibers were stimulated with ATP and/or insulin at indicated concentrations, and 2-NBDG uptake was assayed. *B*: Adult fibers were isolated from mice fed NCD and HFD. 2-NBDG uptake was measured after insulin (100 nmol/L) or ATP (100 μmol/L) stimulation. Values are the mean ± SD. ***P* < 0.001 vs. basal; ††*P* < 0.001 with respect to basal HFD muscle fibers. *C*: In the proposed model, electrical stimulation induces the opening of an ATP extrusion pathway, potentially via pannexin 1 (PnX1) activated by a conformational change of the adjacent dihydropyridine receptor (DHPR). This ATP released to the extracellular medium induces an autocrine activation of P2Y receptors. ATP signals through the βγ subunits of a heterotrimeric G protein to activate PI3K-γ, Akt, AS160, and Rab8A, promoting GLUT4 exocytosis and reducing GLUT4 endocytosis. (A high-quality color representation of this figure is available in the online issue.)

brevis muscles; a similar increase was obtained with 100 nmol/L insulin (Fig. 8*A*). Although neither 10 μmol/L ATP nor 10 nmol/L insulin induced a significant increase, a synergistic effect was evident when applied together (Fig. 8*A*). Interestingly, in muscle fibers obtained from mice fed a high-fat diet, the effect of 100 nmol/L insulin on glucose uptake was not present, but 100 μmol/L ATP produced a significant increase, similar to that of muscle fibers from mice fed the control diet (Fig. 8*B*).

DISCUSSION

We describe here a novel mechanism for GLUT4 translocation and glucose uptake that depends on extracellular ATP released by cultured muscle cells after electrical stimulation (Fig. 8*C*). This stimulus acts via action potentials (23), mimicking the physiological activation of skeletal muscle during exercise. Electrical stimulation is able to elicit a cascade of events triggered by ATP release and binding to P2Y purinergic receptors, followed by activation of the serine/threonine kinase Akt that depends on PI3Kγ. Each of the above-mentioned elements is required for ATP-dependent GLUT4 translocation, revealing an unrealized connection between electrical stimulation and Akt activation that can now be studied in the context of exercise. ATP-dependent GLUT4 translocation to the cell surface is related to an increase in the transporter's exocytosis and a decrease in its endocytosis.

The muscle interstitial ATP concentration increases with muscle contraction (35), and muscle contraction per se is a necessary and sufficient stimulus to significantly raise extracellular ATP (35). Electrical stimulation of the ventral roots increased the dialysate ATP concentration in contracting muscle by 150% (35), reaching micromolar concentrations. The somewhat higher concentration of exogenous ATP required to stimulate glucose uptake is probably needed because ectonucleotidases present in the T-tubule membrane can significantly reduce the effective levels.

Mild electrical stimulation was recently reported to activate the PI3K/Akt signaling and increase glucose uptake in L6 and C2C12 muscle cells (36,37). We here show that exogenously added ATP leads to phosphorylation of the two activator sites on Akt. Contractile activity does not result in tyrosine phosphorylation of IRS1 or associated class I PI3K activation (38) but can lead to Akt phosphorylation (39). Contraction-induced Akt activation can be inhibited by wortmannin or LY294002, consistent with a PI3K-dependent process (7). However, contraction does not activate class IA PI3K (7,38) or class II PI3K (40). It is possible that contraction might activate Akt through class

IB PI3K, an enzyme that is activated by heterotrimeric G-protein–coupled receptors rather than tyrosine kinase-coupled receptors (discussed in 41). Our study shows that ATP engages PI3Kγ to mediate its downstream effect on glucose uptake. PI3Kγ is a well-known target of G-coupled receptors, consistent with ATP signaling via purinergic G-coupled receptors. Indeed, exogenous nucleotides lead to Ca^{2+} mobilization, ERK activation, and gene expression in skeletal muscles through activation of P2×/P2Y receptors (42,43).

A further finding of the current study is that exogenous ATP causes phosphorylation of the Akt substrate AS160. This Rab-GAP is believed to be inactivated upon phosphorylation by upstream kinases, allowing activation of Rab proteins required for GLUT4 translocation to the plasma membrane (31). This pathway has been mapped for insulin-stimulated GLUT4 translocation in insulin-sensitive 3T3-L1 adipocytes (44) and L6 myoblasts (25). In addition to its COOH-terminal Rab-GAP domain, AS160 has six phosphorylation motifs (*RXRXXS**/T*) targeted by, but not exclusively, Akt: Ser318, Ser341, Ser570, Ser588, Thr642, and Ser751 (45,46). Interestingly, we here show that ATP induces phosphorylation of the very same residues. AS160 phosphorylation by AMP-kinase occurs predominantly on residues Ser680, Ser711, Ser761, Ser764, and Ser1135 (47). Although contraction stimulated AS160 phosphorylation at Ser318, Ser341, and Ser751, with a tendency to also increase Ser588, it did not have any evident effect on Thr642 or Ser666 (48). In contrast, ATP led to phosphorylation of Thr642 in the current study, suggesting that more than one pathway is involved in AS160 phosphorylation.

AS160 and the related protein TBC1D1 have been proposed as potential sites for the convergence of insulin and exercise signaling leading to stimulation of glucose transport in skeletal muscle (11,49,50). It is tantalizing to hypothesize that ATP may be an element conveying the insulin-sensitizing effect of exercise by increasing AS160 phosphorylation. We could not study phosphorylation of TBC1D1 because its expression in cultured myotubes is too low to be detected by currently available antibodies.

A further novelty of this study is the revelation that ATP largely promotes GLUT4 exocytosis and partly reduced its endocytosis. The exocytic route likely involves GSV that fuse via TeTx-sensitive SNAREs, such as VAMP2, and GSV traffic is promoted by Rab8A but not Rab10.

Exercise is a potent stimulus that enhances insulin action in skeletal muscle from diabetic patients, and considering that the effects of ATP seen in myotubes were also seen in adult muscle fibers and are still present in an insulin resistance model, this study invites the possibility that extracellular ATP or the signaling pathway it enacts may be tapped upon to design strategies to treat diabetic insulin resistance.

ACKNOWLEDGMENTS

This work was supported by Fondo Nacional de Investigación en Áreas Prioritarias (Chile) 15010006 to E.J. and S.L., Anillo de Investigación Científica y Tecnológica (Chile) ACT1111 to E.J. and S.L., Fondo Nacional de Investigación Científica y Tecnológica (Chile) 11090301 to A.E., Fondo Nacional de Investigación Científica y Tecnológica Postdoc (Chile) 3110170 to A.E.C.-F., Canadian Institutes of Health Research (Canada) MT12601 to A.K., and National Natural Science Foundation (China) #81161120545 and Tianjin Municipal Science and Technology Commission grant #09ZCZDSF04500 to W.N. C.O.-F. was supported by AT-24100067 and UCH0713 Mecesup (Chile). F.A. was supported by AT-24100066.

No potential conflicts of interest relevant to this article were reported.

C.O.-F. and A.E.C.-F. researched data, wrote the manuscript, and approved the final version. F.A. and Q.L. researched data and approved the final version of the manuscript. A.E. contributed to the study design, to analysis and interpretation of data, to drafting and revising the manuscript, and approved the final version. W.N. contributed to the analysis and interpretation of data and approved the final version of the manuscript. S.L. contributed to the study design, to analysis and interpretation of data, and approved the final version of the manuscript. A.K. contributed to the study design, to analysis and interpretation of data, to revising the manuscript, and approved the final version of the manuscript. E.J. contributed to the study design, to analysis and interpretation of data, to writing and revising the manuscript, and approved the final version of the manuscript. E.J. is the guarantor of this work and, as such, had full access to all the data in the study and takes responsibility for the integrity of the data and the accuracy of the data analysis.

This work was previously presented as an abstract in FASEB J:26:Ib715, 2012.

The authors thank Dr. Philip J. Bilan (The Hospital for Sick Children, Toronto) for useful input throughout the course of this study.

REFERENCES

1. Wallberg-Henriksson H, Rincon J, Zierath JR. Exercise in the management of non-insulin-dependent diabetes mellitus. Sports Med 1998;25:25–35
2. Hawley JA, Holloszy JO. Exercise: it's the real thing! Nutr Rev 2009;67:172–178
3. Rose AJ, Richter EA. Skeletal muscle glucose uptake during exercise: how is it regulated? Physiology (Bethesda) 2005;20:260–270
4. Holloszy JO. Exercise-induced increase in muscle insulin sensitivity. J Appl Physiol 2005;99:338–343
5. Pereira LO, Lancha AH Jr. Effect of insulin and contraction up on glucose transport in skeletal muscle. Prog Biophys Mol Biol 2004;84:1–27
6. Kennedy JW, Hirshman MF, Gervino EV, et al. Acute exercise induces GLUT4 translocation in skeletal muscle of normal human subjects and subjects with type 2 diabetes. Diabetes 1999;48:1192–1197
7. Sakamoto K, Hirshman MF, Aschenbach WG, Goodyear LJ. Contraction regulation of Akt in rat skeletal muscle. J Biol Chem 2002;277:11910–11917
8. Douen AG, Ramlal T, Rastogi S, et al. Exercise induces recruitment of the "insulin-responsive glucose transporter". Evidence for distinct intracellular insulin- and exercise-recruitable transporter pools in skeletal muscle. J Biol Chem 1990;265:13427–13430
9. Foley K, Boguslavsky S, Klip A. Endocytosis, recycling, and regulated exocytosis of glucose transporter 4. Biochemistry 2011;50:3048–3061
10. McCarthy AM, Elmendorf JS. GLUT4's itinerary in health & disease. Indian J Med Res 2007;125:373–388
11. Cartee GD, Wojtaszewski JF. Role of Akt substrate of 160 kDa in insulin-stimulated and contraction-stimulated glucose transport. Appl Physiol Nutr Metab 2007;32:557–566
12. Holloszy JO, Narahara HT. Enhanced permeability to sugar associated with muscle contraction. Studies of the role of Ca++. J Gen Physiol 1967; 50:551–562
13. Youn JH, Gulve EA, Holloszy JO. Calcium stimulates glucose transport in skeletal muscle by a pathway independent of contraction. Am J Physiol 1991;260:C555–C561
14. Wright DC, Hucker KA, Holloszy JO, Han DH. Ca2+ and AMPK both mediate stimulation of glucose transport by muscle contractions. Diabetes 2004;53:330–335
15. Fujii N, Jessen N, Goodyear LJ. AMP-activated protein kinase and the regulation of glucose transport. Am J Physiol Endocrinol Metab 2006;291: E867–E877
16. O'Neill HM, Maarbjerg SJ, Crane JD, et al. AMP-activated protein kinase (AMPK) beta1beta2 muscle null mice reveal an essential role for AMPK in

maintaining mitochondrial content and glucose uptake during exercise. Proc Natl Acad Sci U S A 2011;108:16092–16097
17. Witczak CA, Sharoff CG, Goodyear LJ. AMP-activated protein kinase in skeletal muscle: from structure and localization to its role as a master regulator of cellular metabolism. Cell Mol Life Sci 2008;65:3737–3755
18. Merry TL, Steinberg GR, Lynch GS, McConell GK. Skeletal muscle glucose uptake during contraction is regulated by nitric oxide and ROS independently of AMPK. Am J Physiol Endocrinol Metab 2010;298:E577–E585
19. Jensen TE, Wojtaszewski JF, Richter EA. AMP-activated protein kinase in contraction regulation of skeletal muscle metabolism: necessary and/or sufficient? Acta Physiol (Oxf) 2009;196:155–174
20. Ríos E, Pizarro G. Voltage sensor of excitation-contraction coupling in skeletal muscle. Physiol Rev 1991;71:849–908
21. Eltit JM, García AA, Hidalgo J, et al. Membrane electrical activity elicits inositol 1,4,5-trisphosphate-dependent slow Ca2+ signals through a Gbeta-gamma/phosphatidylinositol 3-kinase gamma pathway in skeletal myotubes. J Biol Chem 2006;281:12143–12154
22. Carrasco MA, Riveros N, Ríos J, et al. Depolarization-induced slow calcium transients activate early genes in skeletal muscle cells. Am J Physiol Cell Physiol 2003;284:C1438–C1447
23. Eltit JM, Hidalgo J, Liberona JL, Jaimovich E. Slow calcium signals after tetanic electrical stimulation in skeletal myotubes. Biophys J 2004;86:3042–3051
24. Buvinic S, Almarza G, Bustamante M, et al. ATP released by electrical stimuli elicits calcium transients and gene expression in skeletal muscle. J Biol Chem 2009;284:34490–34505
25. Randhawa VK, Ishikura S, Talior-Volodarsky I, et al. GLUT4 vesicle recruitment and fusion are differentially regulated by Rac, AS160, and Rab8A in muscle cells. J Biol Chem 2008;283:27208–27219
26. Casas M, Figueroa R, Jorquera G, Escobar M, Molgó J, Jaimovich E. IP(3)-dependent, post-tetanic calcium transients induced by electrostimulation of adult skeletal muscle fibers. J Gen Physiol 2010;136:455–467
27. Osorio-Fuentealba C, Valdés JA, Riquelme D, Hidalgo J, Hidalgo C, Carrasco MA. Hypoxia stimulates via separate pathways ERK phosphorylation and NF-kappaB activation in skeletal muscle cells in primary culture. J Appl Physiol 2009;106:1301–1310
28. Li D, Randhawa VK, Patel N, Hayashi M, Klip A. Hyperosmolarity reduces GLUT4 endocytosis and increases its exocytosis from a VAMP2-independent pool in l6 muscle cells. J Biol Chem 2001;276:22883–22891
29. Contreras-Ferrat AE, Toro B, Bravo R, et al. An inositol 1,4,5-triphosphate (IP3)-IP3 receptor pathway is required for insulin-stimulated glucose transporter 4 translocation and glucose uptake in cardiomyocytes. Endocrinology 2010;151:4665–4677
30. Nolte LA, Yarasheski KE, Kawanaka K, Fisher J, Le N, Holloszy JO. The HIV protease inhibitor indinavir decreases insulin- and contraction-stimulated glucose transport in skeletal muscle. Diabetes 2001;50:1397–1401
31. Sun Y, Bilan PJ, Liu Z, Klip A. Rab8A and Rab13 are activated by insulin and regulate GLUT4 translocation in muscle cells. Proc Natl Acad Sci U S A 2010;107:19909–19914
32. Sano H, Roach WG, Peck GR, Fukuda M, Lienhard GE. Rab10 in insulin-stimulated GLUT4 translocation. Biochem J 2008;411:89–95
33. Gonzalez E, McGraw TE. Insulin signaling diverges into Akt-dependent and -independent signals to regulate the recruitment/docking and the fusion of GLUT4 vesicles to the plasma membrane. Mol Biol Cell 2006;17:4484–4493
34. Randhawa VK, Thong FS, Lim DY, et al. Insulin and hypertonicity recruit GLUT4 to the plasma membrane of muscle cells by using N-ethylmaleimide-sensitive factor-dependent SNARE mechanisms but different v-SNAREs: role of TI-VAMP. Mol Biol Cell 2004;15:5565–5573
35. Li J, King NC, Sinoway LI. Interstitial ATP and norepinephrine concentrations in active muscle. Circulation 2005;111:2748–2751
36. Yano S, Morino-Koga S, Kondo T, et al. Glucose uptake in rat skeletal muscle L6 cells is increased by low-intensity electrical current through the activation of the phosphatidylinositol-3-OH kinase (PI-3K) / Akt pathway. J Pharmacol Sci 2011;115:94–98
37. Kim MS, Lee J, Ha J, et al. ATP stimulates glucose transport through activation of P2 purinergic receptors in C(2)C(12) skeletal muscle cells. Arch Biochem Biophys 2002;401:205–214
38. Goodyear LJ, Giorgino F, Balon TW, Condorelli G, Smith RJ. Effects of contractile activity on tyrosine phosphoproteins and PI 3-kinase activity in rat skeletal muscle. Am J Physiol 1995;268:E987–E995
39. Xiao Y, Sharma N, Arias EB, Castorena CM, Cartee GD. A persistent increase in insulin-stimulated glucose uptake by both fast-twitch and slow-twitch skeletal muscles after a single exercise session by old rats. Age (Dordr) 2012 [Epub ahead of print]
40. Soos MA, Jensen J, Brown RA, O'Rahilly S, Shepherd PR, Whitehead JP. Class II phosphoinositide 3-kinase is activated by insulin but not by contraction in skeletal muscle. Arch Biochem Biophys 2001;396:244–248
41. Vanhaesebroeck B, Leevers SJ, Ahmadi K, et al. Synthesis and function of 3-phosphorylated inositol lipids. Annu Rev Biochem 2001;70:535–602
42. Deli T, Szappanos H, Szigeti GP, Cseri J, Kovács L, Csernoch L. Contribution from P2X and P2Y purinoreceptors to ATP-evoked changes in intracellular calcium concentration on cultured myotubes. Pflugers Arch 2007;453:519–529
43. May C, Weigl L, Karel A, Hohenegger M. Extracellular ATP activates ERK1/ERK2 via a metabotropic P2Y1 receptor in a Ca2+ independent manner in differentiated human skeletal muscle cells. Biochem Pharmacol 2006;71:1497–1509
44. Sano H, Kane S, Sano E, et al. Insulin-stimulated phosphorylation of a Rab GTPase-activating protein regulates GLUT4 translocation. J Biol Chem 2003;278:14599–14602
45. Kane S, Sano H, Liu SC, et al. A method to identify serine kinase substrates. Akt phosphorylates a novel adipocyte protein with a Rab GTPase-activating protein (GAP) domain. J Biol Chem 2002;277:22115–22118
46. Mîinea CP, Sano H, Kane S, et al. AS160, the Akt substrate regulating GLUT4 translocation, has a functional Rab GTPase-activating protein domain. Biochem J 2005;391:87–93
47. Treebak JT, Taylor EB, Witczak CA, et al. Identification of a novel phosphorylation site on TBC1D4 regulated by AMP-activated protein kinase in skeletal muscle. Am J Physiol Cell Physiol 2010;298:C377–C385
48. Treebak JT, Frøsig C, Pehmøller C, et al. Potential role of TBC1D4 in enhanced post-exercise insulin action in human skeletal muscle. Diabetologia 2009;52:891–900
49. Kramer HF, Witczak CA, Fujii N, et al. Distinct signals regulate AS160 phosphorylation in response to insulin, AICAR, and contraction in mouse skeletal muscle. Diabetes 2006;55:2067–2076
50. Taylor EB, An D, Kramer HF, et al. Discovery of TBC1D1 as an insulin-, AICAR-, and contraction-stimulated signaling nexus in mouse skeletal muscle. J Biol Chem 2008;283:9787–9796